AIP Advances

Sound reduction by metamaterial-based acoustic enclosure

Shanshan Yao, Pei Li, Xiaoming Zhou, and Gengkai Hu

Citation: AIP Advances **4**, 124306 (2014); doi: 10.1063/1.4902339
View online: http://dx.doi.org/10.1063/1.4902339
View Table of Contents: http://scitation.aip.org/content/aip/journal/adva/4/12?ver=pdfcov
Published by the AIP Publishing

Sound reduction by metamaterial-based acoustic enclosure

Shanshan Yao, Pei Li, Xiaoming Zhou, and Gengkai Hu[a]
Key Laboratory of Dynamics and Control of Flight Vehicle, Ministry of Education and School of Aerospace Engineering, Beijing Institute of Technology, Beijing 100081, China

(Received 1 October 2014; accepted 24 October 2014; published online 18 November 2014)

In many practical systems, acoustic radiation control on noise sources contained within a finite volume by an acoustic enclosure is of great importance, but difficult to be accomplished at low frequencies due to the enhanced acoustic-structure interaction. In this work, we propose to use acoustic metamaterials as the enclosure to efficiently reduce sound radiation at their negative-mass frequencies. Based on a circularly-shaped metamaterial model, sound radiation properties by either central or eccentric sources are analyzed by numerical simulations for structured metamaterials. The parametric analyses demonstrate that the barrier thickness, the cavity size, the source type, and the eccentricity of the source have a profound effect on the sound reduction. It is found that increasing the thickness of the metamaterial barrier is an efficient approach to achieve large sound reduction over the negative-mass frequencies. These results are helpful in designing highly efficient acoustic enclosures for blockage of sound in low frequencies. [http://dx.doi.org/10.1063/1.4902339]

I. INTRODUCTION

Acoustic metamaterials with negative dynamic mass have been considerably developed in the past decade, and one of their main applications is the efficient sound attenuation over low frequency bands.[1–3] Three-dimensional metamaterial structures are firstly proposed and they typically consist of a hard core surrounded with a soft coating and embedded in a rigid matrix.[1] Later developed two-dimensional acoustic metamaterials composed of mass-weighted membranes have the lower mass weight, making them more preferably used in noise isolation.[4,5] The single cell of membrane-type metamaterials blocks sound in a narrow frequency range, but a multi-celled array has been shown to provide multiple peaks in transmission loss.[6] In addition, a simple stretched membrane has very good sound reflection performances below the cutoff frequencies.[7,8] Influences of geometric and material properties of membrane structures on sound reflection have been evaluated by analytic vibro-acoustic models,[9–11] and examined also by numerical and experimental studies.[12–14]

The focus of sound reduction analyses on metamaterials has been largely concentrated on the case where the reflected waves by metamaterial slabs will be radiated to infinity and not coming back to produce additional wave loadings. However, there are many practical systems in which noise sources are contained within a finite volume, and sound radiation control of noise sources by an enclosure (barriers) has the profound significance in engineering applications. Due to the existence of enclosed volume between the source and barrier, the acoustic-structure coupling interaction makes effective sound insulation difficult to realize, especially in the low-frequency regime. This work aims at exploring the possibility of utilizing acoustic metamaterials with negative effective mass to be the sound barrier and to suppress sound radiation at negative-mass frequencies.

[a]Corresponding author. E-mail: hugeng@bit.edu.cn

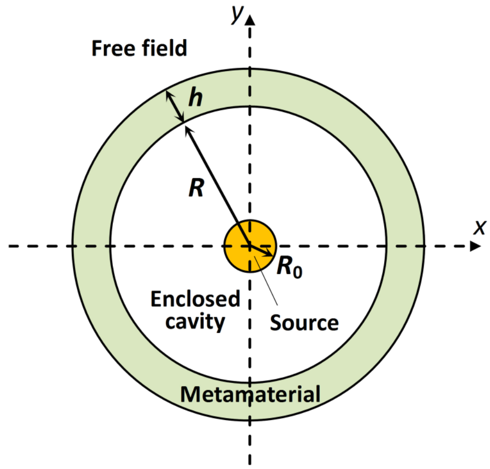

FIG. 1. A circularly-shaped metamaterial with an internal source.

The paper is organized as follows. We introduce the model geometry in Sec. II and provide an analytic model of sound radiation by considering a central source. The structure model of metamaterial barriers is presented in Sec. III and sound reduction analyses are conducted regarding both the central source and eccentric source. Conclusions of the results are laid out in Sec. IV.

II. THE MODEL OF THE PROBLEM

Without the loss of generality, we consider the two-dimensional scenario, as shown in Fig. 1, where a circular cavity of radius R is enclosed by the metamaterial barrier with the thickness h. Acoustics will be radiated from a vibrating cylinder of the radius R_0, which locates at the coordinate origin. The enclosed cavity and external free field are assumed to be the air with the mass density ρ_0=1.25 kg/m^3 and sound velocity c_0=343 m/s.

The barrier will be designed based on the thin-plate acoustic metamaterials, which are characterized by a fluid material with anisotropic effective mass density ρ=diag[ρ_r,ρ_θ]. In the time-harmonic case ($e^{-j\omega t}$), the general expression of acoustic wave equation in the metafluid with anisotropic mass is written as

$$\nabla \cdot \left(\boldsymbol{\rho}^{-1} \nabla p\right) + \frac{\omega^2}{\kappa} p = 0 \tag{1}$$

where κ is the bulk modulus. In polar coordinates, this equation is expressed as

$$\frac{1}{r}\frac{\partial}{\partial r}\left(\frac{r}{\rho_r}\frac{\partial p}{\partial r}\right) + \frac{1}{r^2 \rho_\theta}\frac{\partial^2 p}{\partial \theta^2} + \frac{\omega^2}{\kappa} p = 0 \tag{2}$$

By use of separation of variables, we have $p(r,\theta) = R\,(r) \cdot \Theta\,(\theta)$ and rewrite Eq. (2) as

$$r\frac{\partial}{\partial r}\left(r\frac{\partial P(r)}{\partial r}\right) + \left(\frac{\rho_r}{\kappa}\omega^2 r^2 - \frac{\rho_r}{\rho_\theta} m^2\right) R(r) = 0 \tag{3a}$$

$$\Theta''(\theta) + m^2 \Theta(\theta) = 0 \tag{3b}$$

The solution of Eq. (3a) is the Bessel function of the order $\nu = m\sqrt{\rho_r/\rho_\theta}$. Then the general expression of acoustic pressure is given by

$$p(r,\theta) = \sum_{m=0}^{\infty} J_v(k_r r) e^{im\theta}, \text{ with } k_r = \omega\sqrt{\rho_r/\kappa} \tag{4}$$

From Eq. (4), the particle velocity in the radial direction is obtained as

$$v_r(r,\theta) = \frac{k_r}{j\omega\rho_r}\sum_{m=0}^{\infty} J_v'(k_r r)e^{im\theta} \tag{5}$$

According to Eqs. (4) and (5), the pressure and radial velocity fields in each region of Fig. 1 are given below.

In the enclosed cavity,

$$p = \sum_{m=0}^{\infty}\left[B_m J_m(k_0 r) + A_m H_m(k_0 r)\right]e^{im\theta} \tag{6a}$$

$$v_r = \frac{k_0}{j\omega\rho_0}\sum_{m=0}^{\infty}\left[B_m J_m'(k_0 r) + A_m H_m'(k_0 r)\right]e^{im\theta} \tag{6b}$$

In the metamaterial barrier,

$$p = \sum_{m=0}^{\infty}\left[D_m J_v(k_r r) + C_m H_v(k_r r)\right]e^{im\theta} \tag{7a}$$

$$v_r = \frac{k_r}{j\omega\rho_r}\sum_{m=0}^{\infty}\left[D_m J_v'(k_r r) + C_m H_v'(k_r r)\right]e^{im\theta} \tag{7b}$$

In the free field,

$$p = \sum_{m=0}^{\infty} E_m H_m(k_0 r)e^{im\theta} \tag{8a}$$

$$v_x = \frac{k_0}{j\omega\rho_0}\sum_{m=0}^{\infty} E_m H_m'(k_0 r)e^{im\theta} \tag{8b}$$

where k_0=ω/c_0, A_m, B_m, C_m, D_m, and E_m are unknown scattering coefficients. At interfaces r_1=R and r_2=R+h, the continuous conditions of the pressure and radial velocity result in

$$\begin{pmatrix} A_m \\ B_m \end{pmatrix} = \mathbf{T}\begin{pmatrix} E_m \\ 0 \end{pmatrix} \tag{9}$$

with

$$\mathbf{T} = (\mathbf{M}_1)^{-1}\mathbf{N}_1(\mathbf{N}_2)^{-1}\mathbf{M}_2 \tag{10}$$

where

$$\mathbf{M}_i = \begin{bmatrix} H_m(k_0 r_i) & J_m(k_0 r_i) \\ \dfrac{k_0}{\rho_0}H_m'(k_0 r_i) & \dfrac{k_0}{\rho_0}J_m'(k_0 r_i) \end{bmatrix} \tag{11a}$$

$$\mathbf{N}_i = \begin{bmatrix} H_r(k_r r_i) & J_r(k_r r_i) \\ \dfrac{k_r}{\rho_r}H_r'(k_r r_i) & \dfrac{k_r}{\rho_r}J_r'(k_r r_i) \end{bmatrix} \tag{11b}$$

Acoustic monopole (m=0), dipole (m=1), quadrupole (m=2) will be considered and realized by imposing pressure boundary condition $p_m = I_m e^{im\theta}$ at the interface r=R_0. This condition leads to

$$B_m J_m(k_0 R_0) + A_m H_m(k_0 R_0) = I_m \tag{12}$$

Combining Eqs. (9) and (12) can get that

$$E_m = \frac{I_m}{T_{11}J_m(k_0 R_0) + T_{21}H_m(k_0 R_0)} \tag{13}$$

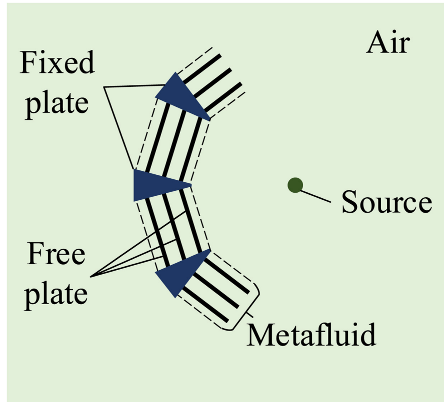

FIG. 2. The structure model of the metamaterial barrier.

The barrier's performance can be characterized by the reduction of pressure level at a far location ($r=R_{\rm far} \gg R+h$) due to the presence of the barrier. For the cylindrical source of the m-th order, the sound reduction SR is expressed as

$$SR = 20 \log \left| \frac{T_{11} J_m(k_0 R_0) + T_{21} H_m(k_0 R_0)}{H_m(k_0 R_0)} \right| \tag{14}$$

III. SOUND REDUCTION ANALYSES ON THE METAMATERIAL ENCLOSER

A. Geometric structures and properties of the metamaterial barrier

The metamaterial barrier we considered is physically realized by circularly arranged rectangular channels filled with thin-plate structures and adjacent channels are separated with the rigid and fixed solid as shown in Fig. 2. In each channel, thin plates of the width 4.8 mm and thickness 9.6 µm are arranged periodically with the lattice constant 3 mm. This structure can be seen as a fluid medium with anisotropic mass density. Since the rigid solids separating the channels are motionless, the annular density of effective fluid is infinite. Due to the vibroacoustic behavior of the clamped layer in the channel, the radial density follows the Drude-medium model, and is expressed as $\rho_e = \rho\left(1-\omega_c^2/\omega^2\right)$. Negative effective radial density can be achieved below the cut-off frequency ω_c, which equals probably the fundamental natural frequency of the clamped plate. The purpose of this work is to verify if the sound reduction is achievable in the negative-mass band when the source is enclosed within the metamaterial barrier.

In the following study, we consider two types of materials for the thin plate: the epoxy (Young's modulus 2.5 Gpa, Poisson's ratio 0.4, and mass density 1400) and aluminum (Young's modulus 70 Gpa, Poisson's ratio 0.33, and mass density 2700). We assume and verify later that effective properties of the circular metamaterial inherit those of the planar system, which can be determined according to the transfer matrix method.[11] The results of effective radial density ρ_e and bulk modulus κ_e are shown in Figs. 3(a) and 3(b) for different number $N=1,3,5$ of epoxy and aluminum plates. It is shown that effective parameters are almost independent on the layer number, meaning that they can be trusted to represent the structured metamaterials. The cut-off frequencies for the epoxy and aluminum plates are respectively 558 Hz and 2166 Hz. In the following sections, we will analyze the sound reduction effect of the circular enclosure made of this metamaterial in the negative-mass region by setting the resonant frequency of the enclosed cavity in between 558 Hz and 2166 Hz.

B. Sound radiation by the central source

We consider the circular enclosure with R=90mm and R_0=9mm. The metamaterial shell consists of three layers of thin plates, and has the thickness h=9mm. It is first noted that the air cavity

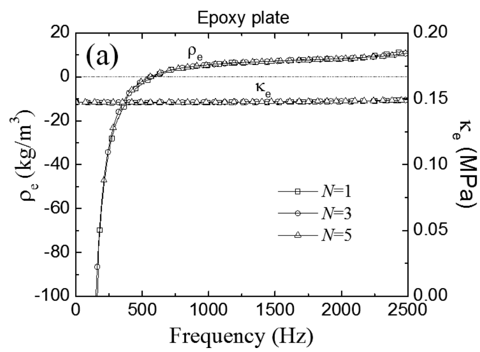

FIG. 3. Effective radial mass density and bulk modulus for the (a) epoxy plate and (b) aluminum plate metamaterials.

enclosed by the rigid wall at $r=R$ and having a nonvanishing pressure distribution at inner boundary ($r=R_0$) will exhibit the fundamental monopolar, dipolar, and quadrapolar resonances at frequencies, 669Hz, 1140Hz, and 1853Hz respectively. These resonant frequencies lie outside the negative mass region for the epoxy-plate metamaterial, while inside the one for the aluminum-plate metamaterial. We will examine if efficient sound reduction is achievable in the negative-mass region for both metamaterial systems.

The sound reductions of the metamaterial barrier under excitations of monopolar, dipolar, and quadrapolar sources are shown in Fig. 4 by the solid circles. The shaded region indicates the frequency band of negative effective mass. For the epoxy-plate metamaterial system (Fig. 4(a)), a remarkable dip of sound reduction can be observed in the negative-mass region for all three types of excitation sources. These are typical results of acoustic-structure interactions, different than the case in an open space, where the negative mass causes always the wave attenuation. We explain the physics of this phenomenon by the insufficient decay length of metamaterials near below the zero-mass frequency. For metamaterials in an open space, zero-mass frequency corresponds almost exactly to the dip in transmission loss, while for the finite space analyzed here, *SR* means zero at zero-mass frequency as if the metamaterial doesn't exist. Sound reduction goes further downwards below the zero-mass frequency due to the small value of decay length, until at the dip frequency, absolute

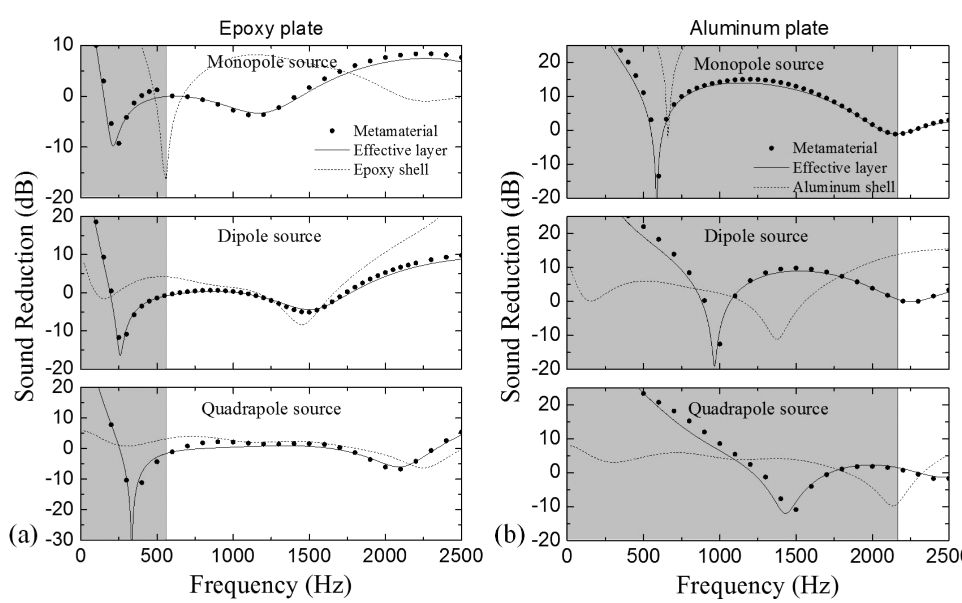

FIG. 4. Sound reduction of the structured metamaterial, their effective medium, and a pure plate under excitations of monopole, dipole, quadrapole sources for (a) epoxy plate and (b) aluminum plate systems.

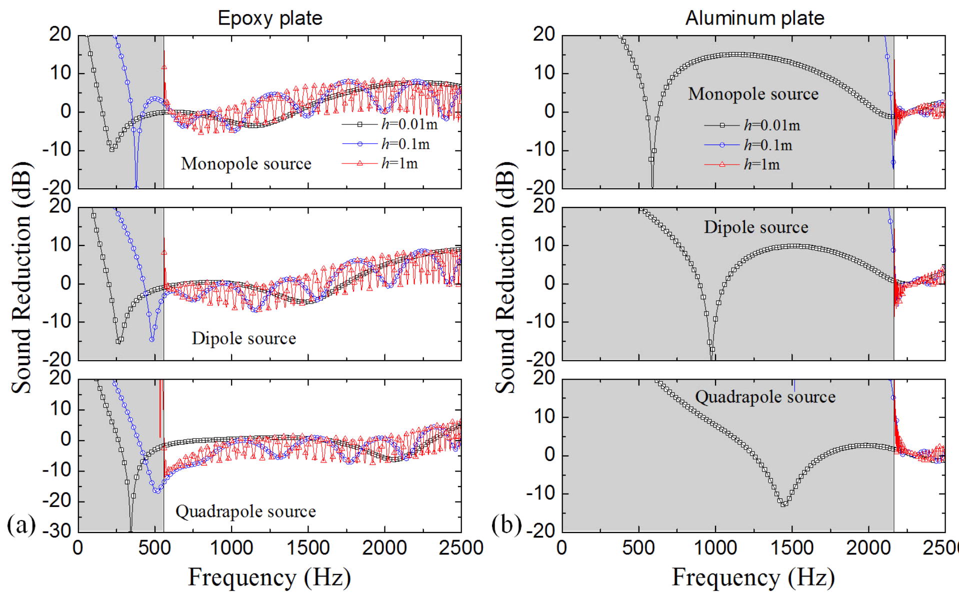

FIG. 5. Sound reduction given by effective medium prediction for various barrier thicknesses h=0.01, 0.1, and 1m in (a) epoxy plate and (b) aluminum plate systems.

values of negative mass are large enough to block the sound radiation. It is worth to note that this phenomenon happens in a general manner regardless of the source types and metamaterial systems with zero-mass frequencies either lower (Fig. 4(a)) or higher (Fig. 4(b)) than the cavity resonant frequencies. It is also significant to compare the sound reduction of the metamaterial barrier and that of a conventional material. The latter material is chosen as the pure epoxy or aluminum plate with the same weight of the plates used in constructing the metamaterial structures, namely the pure plate with the thickness 0.0285mm. The results are shown in Fig. 4 by the dashed lines. In the case of the monopolar source, the bending vibration of the plate is prohibited and the system exhibits weak radiation effect at low frequencies. In this special case, a pure plate is superior to the metamaterial barrier for sound reduction in the low-frequency regime. However for other sources types, the sound reduction of a pure plate is not better than the metamaterial. For the aluminum metamaterial system (Fig. 4(b)), more than 20 dB improvement can be obtained below 500 Hz. We also demonstrate that effective medium predictions (solid line) based on the analytic model developed above match very well the results of actual systems. This makes it more convenient to conduct the parametric analyses on sound reduction by the metamaterial barrier.

Based on the analytic model, we first analyze the influence of the barrier thickness on the sound reduction, as shown in Fig. 5, where three different thicknesses h=0.01, 0.1, and 1m of the barrier are examined. It can be found in any cases that, the dip frequency of sound reduction moves upwards as the thickness increases. This is because that the decay length has been enhanced by the increased physical size of the metamaterial. In the special case of h=1m, the band of efficient sound reduction has been defined exactly by the negative-mass frequencies. This example shows that the barrier thickness has a profound influence on the sound reduction of the metamaterial. Studied in the second example is the effect of the cavity size, as shown in Fig. 6, where three different cavity radii R=R_0, 3 R_0, 5 R_0 are chosen. The case of R=R_0 means no existence of the cavity, and is the case where the dip frequency is closest to the zero-mass frequency. The presence of the cavity will inevitably drop down the dip frequency. The result suggests that the cavity size needs to be diminished as small as possible for efficient sound reduction.

C. Sound radiation by the eccentric source

This section will deal with the case where the source origin $S(x_0\neq 0, y_0=0)$ is offset from the origin $O(0,0)$ of the circular barrier. In this case, the sound reduction is non-uniform among

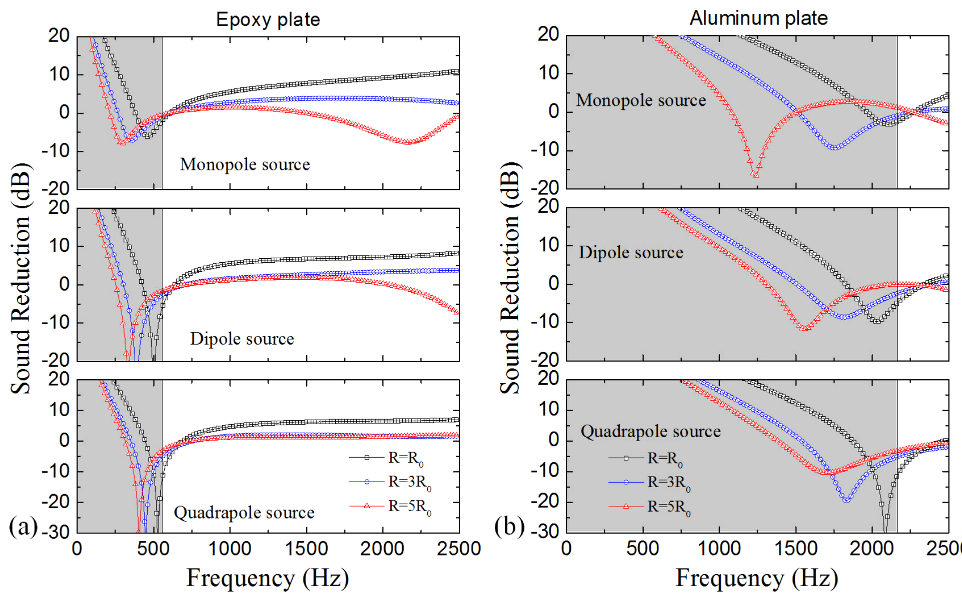

FIG. 6. Sound reduction given by effective medium prediction for various cavity sizes R=R_0, 3 R_0, 5 R_0 in (a) epoxy plate and (b) aluminum plate systems.

different directions, and we examine only the maximum sound radiation measured in the *OS* direction. Figure 7 shows the sound reduction of the aluminum-plate metamaterial barrier (solid circles) in the case of the eccentricity x_0=45mm. Multiple dips in sound reduction appear in the negative-mass region. Relative to the pure aluminum plate (dashed lines), efficient sound reduction is achievable below the first dip frequency except the monopole source case. Although the developed analytical model is invalid here, effective medium predictions can still be provided based on

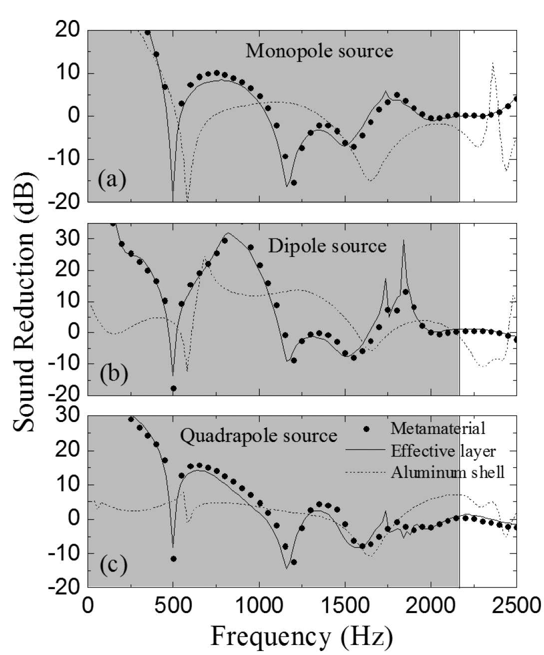

FIG. 7. Sound reduction of the structured metamaterial, their effective medium, and a pure plate under excitations of monopole, dipole, quadrapole sources for the aluminum plate system with the eccentricity x_0=45mm of the source.

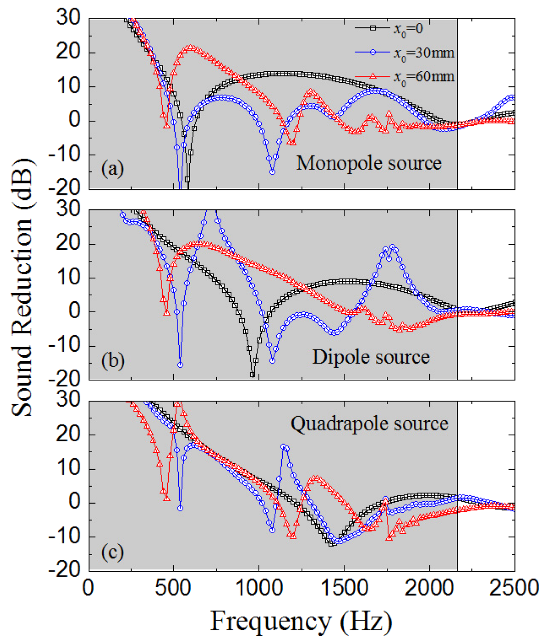

FIG. 8. Sound reduction given by effective medium prediction for various eccentricity x_0=0, 30, 60mm of the source in the aluminum plate system.

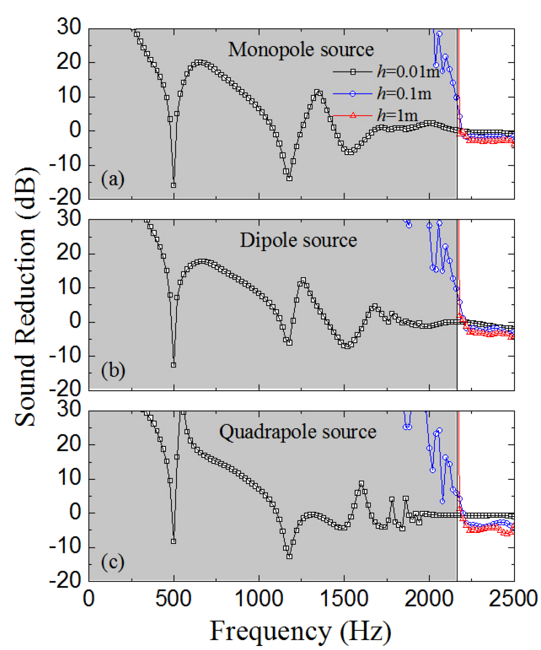

FIG. 9. Sound reduction given by effective medium prediction for various barrier thicknesses h=0.01, 0.1, and 1m in the aluminum plate system with the eccentricity x_0=45mm of the source.

the simulation for a homogeneous medium with effective parameters, as shown by the solid line, and are in good agreement with the actual results.

As seen in Fig. 7, a fundamental property of sound radiation by an eccentric source is that the first dip frequency becomes insensitive to the source type. This is more clearly evidenced in Fig. 8, where sound reductions are given by effective medium predictions for different eccentricities x_0=0, 30, 60mm. In the central source case (x_0=0), the angular distribution of the radiated acoustic fields is uniquely dependent on the type of source due to the symmetry of the system. Hence the first dip frequency of the coupled system becomes higher for higher order of multipole sources. The system symmetry will be broken in the presence of an eccentric source, and the radiation fields of asymmetric modes can be excited with any types of sources. It is seen in Fig. 8 that the first dip frequency remains almost unchanged against the variation of the eccentricity and localized near the dip frequency in case of the central monopole source.

The effect of the barrier thickness on the sound radiation of an eccentric source with x_0=45mm is illustrated in Fig. 9, where three different thicknesses h=0.01, 0.1, and 1m are considered. It is found that the frequency band of efficient sound reduction can be greatly expanded with the increasing of the barrier thickness and overlaps with the negative mass band under case of a sufficiently large thickness. We therefore conclude that increasing the barrier thickness to enhance the sound reduction is robust against variations of the type and the eccentricity of the source.

From above analyses, it is quite evident that sound reduction behaviors of metamaterials covering a finite volume of cavity are more complex than the case in an open space. Due to the acoustic-structure interaction, sound reduction at low frequency is closely related to the barrier thickness, the cavity size, the source type, and the eccentricity of the source. Their fundamental correlations have been discovered by these preliminary studies. More analyses have to be conducted for the practical system of interest.

IV. CONCLUSIONS

Based on a circularly-shaped metamaterial model, we study the sound reduction property of the metamaterial enclosure with an internal source. It has been demonstrated that a remarkable dip in sound reduction always exists in the negative-mass band for a metamaterial with small thickness. In the central source case, the dip frequency increases as the multipole source of higher order is considered, while in the presence of a nonzero eccentricity of the source, it remains almost unchanged against the variation of the source type and eccentricity. Increasing the barrier thickness is found to be the most effective approach to achieve efficient sound reduction over the entire negative-mass band. Though based on an idealized model, the obtained results reveal features common to more complex systems in practice. They are potentially useful in designing highly efficient metamaterial-based acoustic barriers.

ACKNOWLEDGMENTS

This work was supported by the National Natural Science Foundation of China (Grant Nos. 11072031, 11302028, and 11221202), the National Basic Research Program of China (Grant No. 2011CB610302), and Program for New Century Excellent Talents in University (Grant No. NCET-11-0794).

[1] Z. Liu, X. Zhang, Y. Mao, Y. Y. Zhu, Z. Yang, C. T. Chan, and P. Sheng, Science **289**(5485), 1734–1736 (2000).
[2] S. Yao, X. Zhou, and G. Hu, New J. Phys. **10**(4), 043020 (2008).
[3] H. H. Huang and C. T. Sun, New J. Phys. **11**(1), 013003 (2009).
[4] Z. Yang, H. M. Dai, N. H. Chan, G. C. Ma, and P. Sheng, Appl. Phys. Lett. **96**(4), 041906–041903 (2010).
[5] Z. Yang, J. Mei, M. Yang, N. Chan, and P. Sheng, Phys. Rev. Lett. **101**(20), 204301 (2008).
[6] C. J. Naify, C.-M. Chang, G. McKnight, F. Scheulen, and S. Nutt, J. Appl. Phys. **109**(10), 104902–104909 (2011).
[7] S. H. Lee, C. M. Park, Y. M. Seo, Z. G. Wang, and C. K. Kim, Phys. Lett. A **373**(48), 4464–4469 (2009).
[8] S. Yao, X. Zhou, and G. Hu, New J. Phys. **12**(10), 103025 (2010).
[9] Y. Zhang, J. Wen, Y. Xiao, X. Wen, and J. Wang, Phys. Lett. A **376**(17), 1489–1494 (2012).
[10] Y. Chen, G. Huang, X. Zhou, G. Hu, and C.-T. Sun, J. Acoust. Soc. Am. **136**(3), 969–979 (2014).
[11] P. Li, S. Yao, X. Zhou, G. Huang, and G. Hu, J. Acoust. Soc. Am. **135**(4), 1844–1852 (2014).
[12] C. J. Naify, C.-M. Chang, G. McKnight, and S. Nutt, J. Appl. Phys. **108**(11), 114905–114907 (2010).
[13] C. J. Naify, C.-M. Chang, G. McKnight, and S. Nutt, J. Appl. Phys. **110**(12), 124903–124908 (2011).
[14] C. J. Naify, C.-M. Chang, G. McKnight, and S. R. Nutt, J. Acoust. Soc. Am. **132**(4), 2784–2792 (2012).